https://doi.org/10.5194/esurf-2020-92
Preprint. Discussion started: 16 December 2020

The formation processes and development characteristics of sandbars due to outburst flood triggered by landslide dam overtopping failure

Xiangang Jiang✉[1] · Haiguang Cheng[1] · Lei Gao[2] · Weiming Liu[3]

[1]College of Civil Engineering, Sichuan Agricultural University, Dujiangyan, Chengdu 611830, China

[2]Key Laboratory of Ministry of Education for Geomechanics and Embankment Engineering, Hohai University, Nanjing 210098, China

[3]Key Laboratory of Mountain Hazards and Earth Surface Process, Institute of Mountain Hazards and Environment, Chinese Academy of Sciences, Chengdu 610041, China

Correspondence to: Xiangang Jiang (✉E-mail: jxgjim@163.com)

Abstract

Sandbars are an essential form of riverbed morphology which could be affected by landslide dams. However, few studies have focused on the formation processes and development characteristics of sandbars triggered by outburst flood. In such a way, eight group dam failure experiments with 4 to 7 times of dam length movable bed is carried out to study the temporal and spatial distributions of 25 sandbars along the riverbeds, the sandbars geometric characteristics, and the influence of outburst flow hydraulic characteristics on developments of sandbars. The results show that sandbars are formed after peak discharge of outburst flow. The number of sandbars is 0.4 to 1.0 times the ratio of river bed length to dam length. Besides, sandbars have the characteristic of lengthening towards upstream during the failure process. Sandbars'

https://doi.org/10.5194/esurf-2020-92
Preprint. Discussion started: 16 December 2020

upstream edges have a more extensive development than sandbars downstream edges. The length of a sandbar along the channel changes faster than the sandbar's width and height. The sandbars' length and width are about 10 to 80 and 1 to 7 times of average height, respectively, and the average heights of sandbars are about 1 to 3.5 times the maximum particle size. Sandbars' lengths make a more significant impact on sandbars' volumes than widths and heights. It found that the Froude number has a significant influence on the sediment carrying capacity. And the sediment concentrations in volumes of the outburst flow at the upstream edges of all sandbars are greater than those at the downstream edges of sandbars. Meanwhile, the sediment carrying capacities of the outburst flow at the upstream edges of sandbars are smaller than those at the sandbars' downstream edges. And the differences between the sediment concentrations and the sediment carrying capacities determine the sedimentation or entrainment. The results can reference the research on the river channel's geomorphological characteristics affected by the outburst flood.

Keywords

Landslide dam · Overtopping failure · Sediment transport · Sandbar formation and development

1. Introduction

Activities such as rainfalls and earthquakes often cause collapses, landslides, which block the river to form a water retaining body similar to a reservoir dam, called a landslide dam (Takahashi, 2007). According to statistics, 85 % of the dams were destroyed within one year after formations, and more than 50 % of the dams were damaged by overtopping (Costa and Schuster, 1988). Overtopping outburst floods are extraordinarily destructive and seriously threaten people's personal and property safety. Therefore, more and more scholars pay attention to the failure mechanisms and modes of landslide dams and analyze outburst flood hydraulic characteristics and flood evolution process (Pickert et al., 2011; Fan et al., 2012; Jiang et al., 2017, 2018, 2019a; Zhang et al., 2019; Jiang and Wei, 2019b). Indeed, the outburst flood formed by landslide dam failure carries loose materials in the channel during its evolution and erodes and deposits along the channel. Sandbars are one typical landform formed during the outburst flood evolution (Turzewski et al., 2019; Jiang and Wei, 2020; Wu et al., 2020). Sandbars are shaped siltation bodies with exposed water surfaces formed by rivers, lakes, and seashores (Chien et al., 1987). Moreover, sandbars are a feature of the transition zone between aquatic and terrestrial, which have essential impacts on transportation and species habitation using river corridors (Lin, 1990; Tracy-Smith et al., 2012; Alexander et al., 2020). Consequently, sandbars have become the focus of attention on river bedform and ecology.

At present, many researches about formations and developments of sandbars have been conducted in natural rivers. Through field observations and indoor experiments, sandbars' shapes and sizes can be observed intuitively, which is vital for understanding formations and development characteristics of sandbars (Chien et al., 1987; Ashworth, 1996; Ashworth et al., 2000; Wright and Kaplinski, 2011; Demirci et al., 2014; Xie et al., 2017; Alexander et al., 2020). For example, Chien et al. (1987) based on a large number of field cases and data, and concluded that there are three basic types of

https://doi.org/10.5194/esurf-2020-92
Preprint. Discussion started: 16 December 2020

sandbars developments: (1) in the upstream backwater sections and the downstream widening sections of the sandbars, sediments fall to promote the developments of sandbars; (2) water flow erodes the front edges and sides of sandbars, and bends the bars; (3) the protruding river core bedrock forces the flow to diverge and deposit the sediments. Ashworth et al. (2000) through observing the nearly 1 km long sandbar of the Jamuna River in Bangladesh, and sandbars' formation and development process were analyzed. They pointed out that the cross-level formed by dunes and slip face accretion at bar margins dominated developments of sandbars; Wright and Kaplinski (2011) measured the three-dimensional flow structures and sandbars dynamics of the two basins of the Colorado River in the Grand Canyon during the controlled flooding of the Glen Canyon Dam. They found that the lateral reflux zone is conducive to fine particle sediment deposition to form sandbars. Hooke and Yorke (2011) used remote sensing images to analyze sandbars' dynamic evolution processes at multiple time scales. They considered that the developments of sandbars are related to flow hydraulic property. And they pointed out that analyzing the dynamic characteristics of sandbars in rivers over a long period of time still needs more field data; Demirci et al. (2014) obtained the dimensionless equation of sandbars' volumes through experimental data using linear regression and nonlinear regression methods. The results showed that experimental data are in good agreement with the proposed equation, but there was no in-depth analysis of sandbars' other geometric features, and the relationship between the geometric dimensions of sandbars was not clear; Xie et al. (2017) studied the sandbars at the estuary of the Qiantang River and stated that the flow discharge played a major role in sandbars' growths: when the flow discharge was large, the sandbars would be eroded; when the flow discharge was small, the sandbars would be silted.

Some researchers have established mathematical models to simulate sandbars growths and analyzed the development processes of sandbars. For example, Gao (1999) believed that sandbars are the sedimentation results and used the hydrodynamic method to derive the theoretical formula for sandbars' lengths. However, the method is not suitable for unsteady flow, such as outburst flood caused by dammed lake overtopping failure; Defina and Andrea (2003) established a two-dimensional finite element channel morphological evolution model based on a non-cohesive river bed to simulate formations and growths of sandbars. Using this model to study the impact of initial disturbances on the initial flow field, which in turn affected sandbars growths; later, Crosato and Mosselman (2009) simplified the physical mechanism of sandbars formations and established a sandbar formation model. They considered that sandbars' positions would change when the flow discharge changed or the riverside line was eroded or deposited. And they proposed a quantitative method to predict the number of sandbars in the river. But this model is suitable for rivers with a width height ratio less than 100; Mueller and Grams (2018) coupled a simple morphological dynamics model with flow and sediment concentration data, and it could reasonably predict sandbars' volumes change. This method is aimed at the sandbars formed by the debris flow, but the applicability of the sandbars formed by outburst flood remains to be investigated.

Sandbars formed after the landslide dam failure are caused by the strong unsteady outburst flood. Kobayashi et al. (2010) established a two-dimensional morphological

https://doi.org/10.5194/esurf-2020-92
Preprint. Discussion started: 16 December 2020

dynamics model to study sandbars' growth processes under the action of unsteady flow. And they discussed that flow unsteady property seemed to change the growth mechanism of sandbars. Besides, for this type of sandbars, the upstream sediment is mainly supplied by the dam material, which is different from other types of sandbars. Until now, there is little field observation data of riverbed topography during landslide dam breaching. As a result, questions remain regarding the formation processes and development characteristics of the sandbars formed by outburst floods.

Overtopping failure is the most common failure mode of the landslide dam, so this paper investigates the formation processes and growth characteristics of the sandbars formed by the outburst flood due to landslide dam overtopping failure. This paper focuses on the formation processes, the geometrical size characteristics of sandbars in the downstream channel during the dammed lake's failure, and how the outburst flood affects sandbars' developments. Firstly, through flume experiments, sandbars' formation processes on the downstream channel under the dammed lake failure condition were reproduced. Then, based on the experimental data, the growth characteristics of sandbars' upstream and downstream edges were analyzed. Furthermore, statistical analysis of sandbars geometrical dimensions at each moment during the failure process, such as length, width, height, and volume, had been carried out to obtain sandbars' size characteristics. Finally, by combining the hydraulic characteristics of outburst flow at sandbars areas and sediment transport theory, the sandbars' growth mechanisms were analyzed.

https://doi.org/10.5194/esurf-2020-92
Preprint. Discussion started: 16 December 2020

Earth Surface Dynamics Discussions
Open Access

2. Experimental design

2.1 Model design and experimental materials

The longitudinal profiles of experimental landslide dams were trapezoidal and triangular. The trapezoidal dam height and crest width were both 0.3 m, and the triangular dam height was also 0.3 m. In the experiment, river bed slope angle θ was fixed at 10°, and the landslide dam upstream slope angle α was set to 40°, and the landslide dam downstream slope angles β were set to five different values. The moveable bed was set downstream of the model dam, which had a length of 8 m. The downstream channel bed's length was about 4 to 7 times of dam length along the channel. The test parameters are shown in Table 1.

Table 1 test parameters

No.	**Dam shape**	$\boldsymbol{\beta}$ **(°)**
T1	Trapezoid	10
T2	Trapezoid	15
T3	Trapezoid	20
T4	Trapezoid	25
T5	Trapezoid	30
T6	Tringle	10
T7	Tringle	15
T8	Tringle	20

Peng and Zhang (2012) proposed that landslide dam height (H_d), dam bottom width parallel to the channel (W_d), dam volume (V_d), and reservoir volume (V_l) are the key geometric parameters of landslide dam, and proposed a set of dimensionless numbers, $\frac{H_d}{W_d}$, $\frac{V_d^{1/3}}{H_d}$ and $\frac{V_l^{1/3}}{H_d}$, to verify whether the established dam model is consistent with the landslide dam in the field (Zhou et al., 2019). As the field data show that the $\frac{H_d}{W_d}$, $\frac{V_d^{1/3}}{H_d}$ and $\frac{V_l^{1/3}}{H_d}$ are ranged about 0.001 to 2, 0 to 40, and 0 to 20 for filed landslide dam (Zhou et al., 2019). Table 2 shows the dimensionless numbers of

https://doi.org/10.5194/esurf-2020-92
Preprint. Discussion started: 16 December 2020

the experimental dams, which are all within the acceptable range of the field landslide dams, indicating that the dams in the experiments are relatively close to field landslide dams.

Table 2 landslide dam parameters. The value of $\frac{H_d}{W_d}$ ranges from 0.1 to 0.3, and $\frac{V_d^{1/3}}{H_d}$ and $\frac{V_l^{1/3}}{H_d}$ both range from 1 to 2, which all fall within the acceptable range of values of the field landslide dams (Zhou et al., 2019).

No.	H_d (m)	W_d (m)	$\frac{H_d}{W_d}$	$\frac{V_d^{1/3}}{H_d}$	$\frac{V_l^{1/3}}{H_d}$
T1	0.3	2.359	0.127	1.643	1.477
T2	0.3	1.777	0.169	1.513	1.477
T3	0.3	1.482	0.202	1.437	1.477
T4	0.3	1.301	0.231	1.387	1.477
T5	0.3	1.177	0.255	1.350	1.477
T6	0.3	2.059	0.146	1.508	1.477
T7	0.3	1.477	0.203	1.350	1.477
T8	0.3	1.182	0.254	1.254	1.477

The dam materials used in this study were mixtures of sand and graves, with a median particle size D_{50} of 3.8 mm. Due to the flume space limitation, the maximum sediment particle size was set to 20 mm. The riverbed was movable, which consisted of the same material as the dam model. The thickness of the riverbed was set to 0.06 m. The gradation curve of material particles' sizes is shown in Fig. 1.

https://doi.org/10.5194/esurf-2020-92
Preprint. Discussion started: 16 December 2020

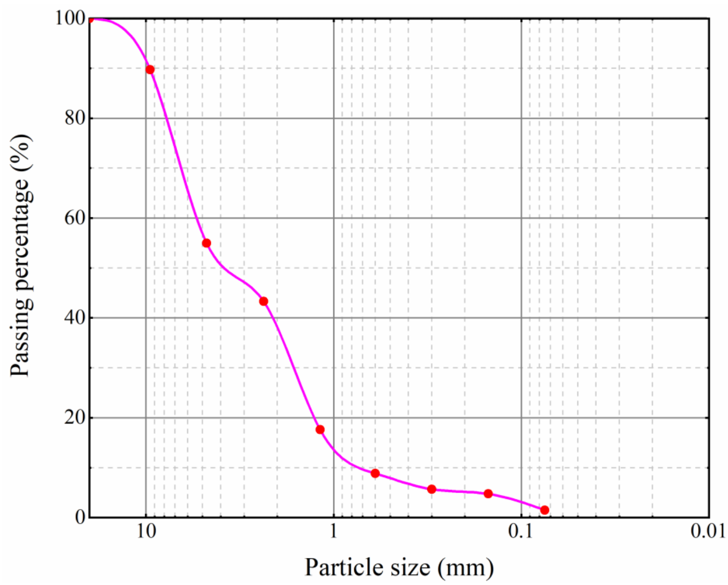

Figure. 1 Gradation curve of the dam materials

2.2 Experimental apparatus

The experimental setups are shown in Fig. 2. The flume was 15 m long, 0.3 m wide, and 0.6 m high. The flume slope was adjustable from 10 to 30°. One side of the flume was transparent glass, and scale lines were drawn on the glass to facilitate observation and recording of experimental phenomena. The inflow discharge was set as 1.0 L s^{-1}. Under the control of the electromagnetic flowmeter, the error range could be controlled within ±0.01 L s^{-1}. During the tests, the toe of the dam upstream slope was set at 4.5 m away from the water supply tank. A baffle with a height of 6 cm was set at the flume end as a boundary condition. Seven cameras were placed on the transparent glass side of the flume, one camera was placed on the top of the dam, and one camera was placed directly behind the flume. A total of nine cameras recorded the whole experimental phenomena.

https://doi.org/10.5194/esurf-2020-92
Preprint. Discussion started: 16 December 2020

Earth Surface Dynamics Discussions
Open Access

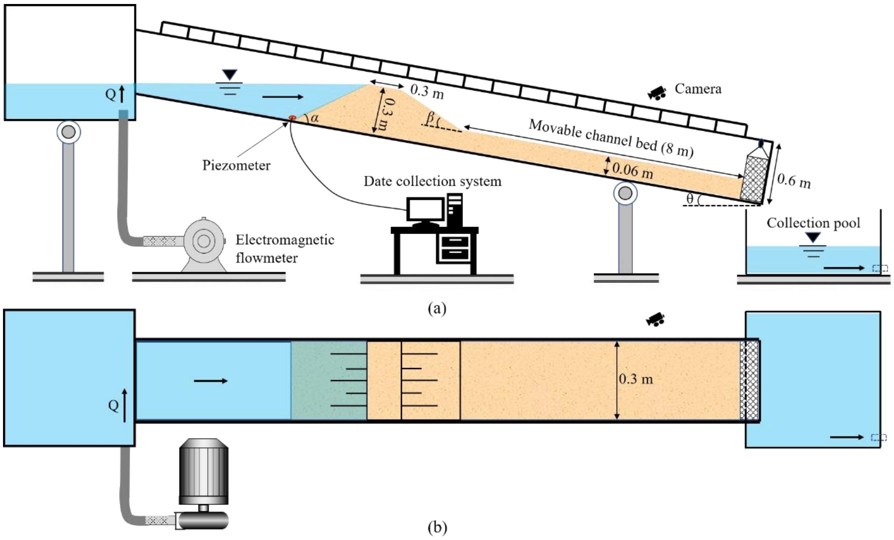

Figure. 2 Experimental setups. (a) Front view of the flume. (b) Top view of the flume.

2.3 Measurements

In the experiment, the flow velocity was measured based on the reference object. After the dam failure, a large number of small balls were continuously thrown into the flume. Because the balls were of small mass and were eye-catching and easy to observe, they would maintain the same movement state as the outburst flow under the flow's drive. In a certain period, the balls' distance can be determined by the glass's scale lines and then divide by the time to get balls' speeds, that is, the outburst flow velocities. Flow depth could be read directly through the glass's scale lines, and the difference between the flow surface elevation and the bed sand elevation represented flow depth.

Sandbars' lengths, widths, and heights could be obtained from the screen. It should be noted that, due to the irregular shapes of the sandbars, the lengths of the sandbars along the flume could be measured, but sandbars' widths and heights were different at different locations. In this paper, the representative width and height values, which were the arithmetic means along the channel, were used. Regarding the sandbars' volumes, according to the actual sandbars' geometric characteristics, the sandbars were divided into several parts, and then the volume calculation formula of the similar geometric body was used to calculate the volume of each part respectively, and finally, the sandbars' volumes were obtained by summing.

3. Experimental results

3.1 Formation processes of sandbars

The outburst flood due to the dam overtopping failure carried the downstream channel's sediment and promoted formations and developments of sandbars. It showed that three to four sandbars downstream the dam after the dam failure. Turzewski et al. (2019) investigated the sandbars in the Yigong River triggered by the Yigong outburst flood in 2000. They found that the number of sandbars is about 0.69 to 0.77 times the ratio of river bed length to dam length for the sandbar frequent region. In this study, sandbars were distributed in the 8 m length of the channel, which is 4 to 7 times of dam length. It reflected the number of sandbars was 0.4 to 1.0 times the ratio of river bed length to dam length. By comparing the experimental data and the field data of Turzewski et al. (2019), it can be found that field data falls within the range of experimental data. Experimental models took more influencing factors into account, while the field data of Turzewski et al. (2019) only focused on the sandbars in the Yigong River case, which is the reason for that field data falls within the range of experimental data.

https://doi.org/10.5194/esurf-2020-92
Preprint. Discussion started: 16 December 2020

It took the T7 test as an example to analyze sandbars formation processes, as shown in Fig. 3. Start timing when the flow just exceeded the dam crest, and at the initial dam failure stage, the outburst flood carried the dam material to the dam downstream slope (T=5 s). As the dam failed further, the flow discharge increased, and outburst flood carried many dam materials to the channel bed (T=19 s). It should be noted that although a large number of sediments were transported on the channel bed before the peak discharge, no sandbar would be formed on the downstream channel bed. After the moment of peak discharge, the flow discharge gradually weakened, and dam materials were transported to the section near the dam toe. The flow could not transport all the sediments away, and some sediments gradually silted down, then the first sandbar occurred near the dam toe (T=30 s, the sandbar in the figure is marked with a blue dotted line). After the first sandbar was formed, flow movement was changed. The advancing flow bypassed the first sandbar, and the flow streamlines bent. Due to inertia, the moving sediments no longer moved along the curved streamline but moved in the original direction. On the opposite side of the first sandbar, sediments piled up to form the second sandbar. With the first and second sandbars' existence, the flow streamline's bending was more apparent, and flow moved along the "S" shaped path to the downstream channel bed. It could be seen that there was a mutual feeding relationship between sandbars and flow. That is, sandbars and flow influenced each other.

Similarly, the first and second sandbars affected the formation of the sandbar downstream. Because of the accumulation and erosion of sediments, the channel bed's sandbars kept growing, and sandbars' locations and geometric dimensions were

https://doi.org/10.5194/esurf-2020-92
Preprint. Discussion started: 16 December 2020

changed. For example, when T=33 s, more and more sediments were deposited on the upstream sandbars' edges, the sandbar near the dam toe continued to grow, and the upstream sandbar's volume increased. When the dam was failed entirely, the sandbars had changed significantly compared to the initial sandbars, making the channel bed topography changed significantly. Eventually, sandbars were scattered on both sides of the flume, forming a meandering channel downstream (T=40 and 47 s). This phenomenon is in good agreement with the field sandbars along the Yigong river (Wu et al., 2020).

Figure. 3 The riverbed morphology at six different moments during the sandbars' formations and growths for the T7 experiment. The sandbars in the figure are marked with blue dotted lines.

3.2 Position characteristics of the sandbars' edges

Figure. 4 shows sandbars' locations on the channel bed during the dam failure. The red lines in the figure represent the sandbars, and the orange rectangles represent the flumes. Figure. 4 can clearly show the formation sequences of sandbars at different locations. That is, sandbars were formed first near the dams, and the farther from the dam toe, the later the sandbar was formed, which is consistent with the content of Sect. 3.1. Sandbars near the downstream dam toes are all located on the dam breach side

https://doi.org/10.5194/esurf-2020-92
Preprint. Discussion started: 16 December 2020

across the river. This characteristic has also been found in Chen et al. (2015).

According to the sandbars' formation sequences, the channel bed's sandbars were divided into three types: the sandbar near the dam toe, the sandbar near the middle reaches, and the sandbar near the bed end. And the characteristics of the position changes of the sandbars' upstream and downstream edges were analyzed, respectively. Figure 4 that the upstream edges of the sandbars near the dam toes in the eight group experiments basically moved upstream with time. But the movement directions of the downstream edges of the sandbars near the dam toes showed diversity: in the two tests of T2 and T5, the sandbars' downstream edges moved toward the dam toes, from a distance from the downstream toe of 3.3 to 2.9 m and 3.7 to 3.5 m respectively, as shown in Fig.4(b) and (e); in the tests of T1, T6, T7, and T8, the sandbars' downstream edges first moved away from the dam toes and then moved toward the dam toes, and the downstream edges move forward compared to the original location. However, the distance they moved is 0.15 to 0.7 m, which is small as shown in Fig.4(a), (f), (g), and (h); in the experiments of T3 and T4, the sandbars' downstream edges positions remained almost unchanged, see Fig.4(c) and (d). However, no matter how the downstream edge positions of the sandbars near the dam toes changed, the results of the eight tests have a common feature: compared with the position when the sandbars were formed, the downstream edges moved less distance, and the amount of movement was much smaller than those of sandbars' upstream edges. The lengths of the sandbars near the dam toes increased with the failure time. It can be seen that the sediments on the sandbars' upstream edges played a greater role in the length developments of the

https://doi.org/10.5194/esurf-2020-92
Preprint. Discussion started: 16 December 2020

sandbars near the dam toes.

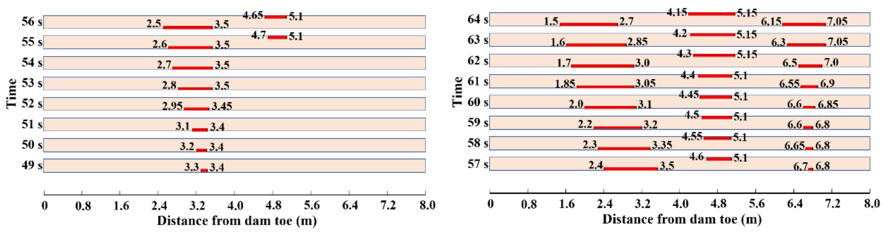

(a)

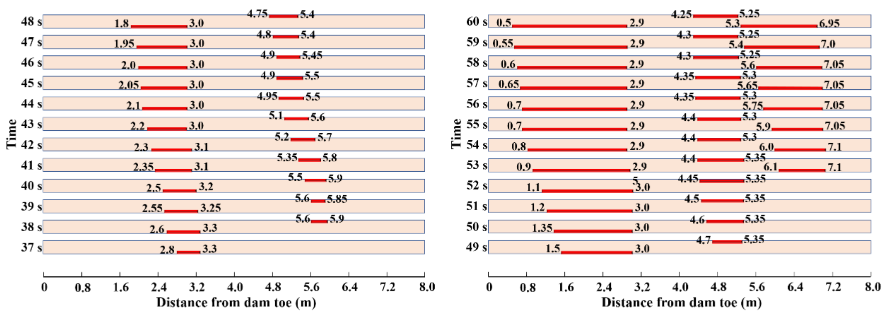

(b)

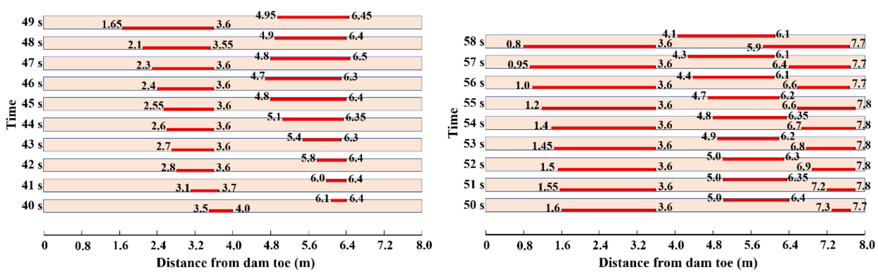

(c)

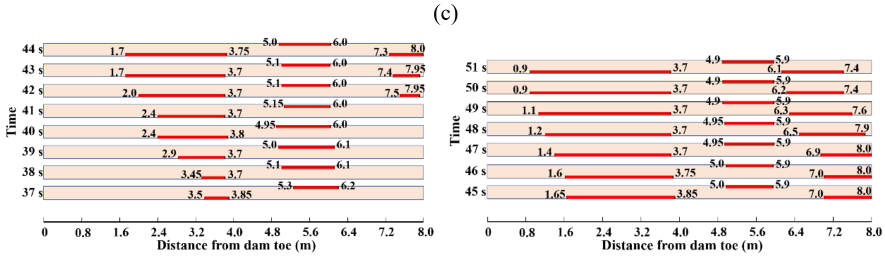

(d)

https://doi.org/10.5194/esurf-2020-92
Preprint. Discussion started: 16 December 2020

Earth Surface Dynamics
Discussions

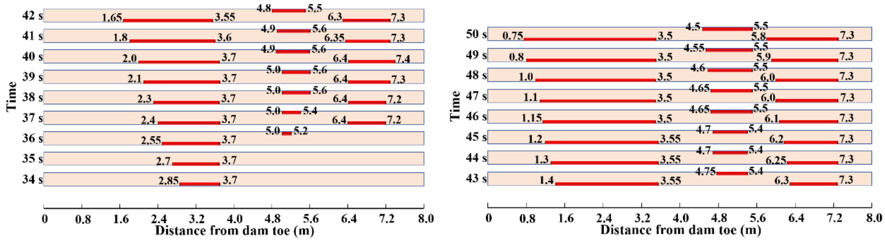

(e)

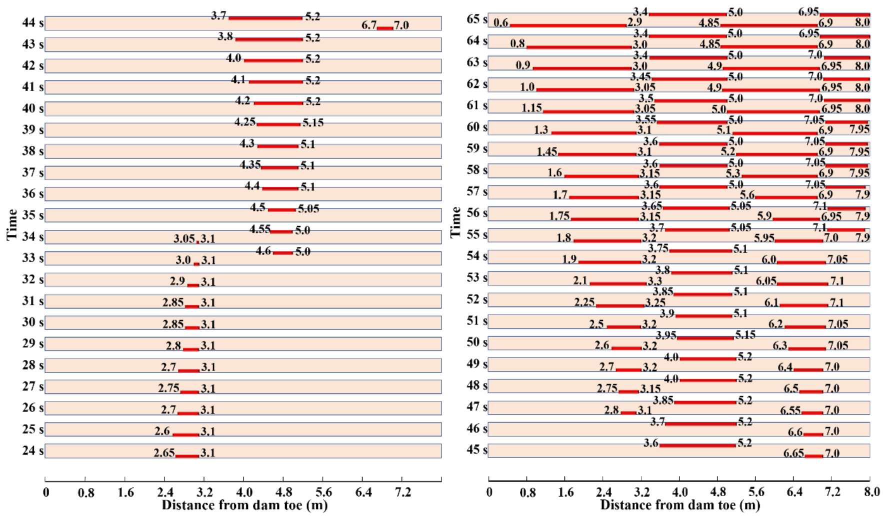

(f)

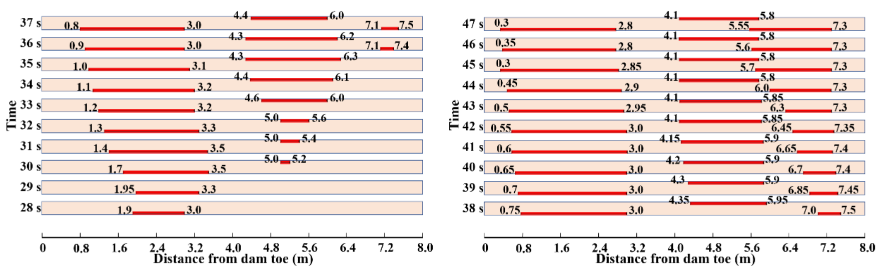

(g)

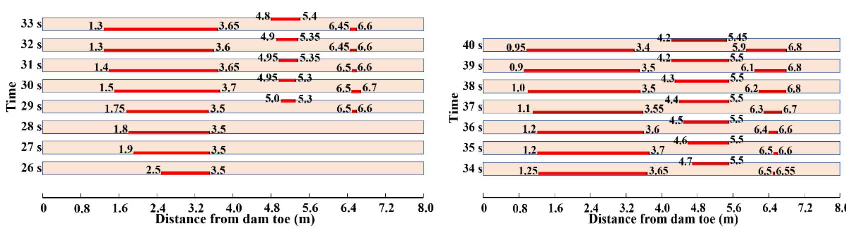

(h)

https://doi.org/10.5194/esurf-2020-92
Preprint. Discussion started: 16 December 2020

Figure. 4 The sandbars' locations during the dam failure: (a) sandbars' locations of the T1 test; (b) sandbars' locations of the T2 test; (c) sandbars' locations of the T3 test; (d) sandbars' locations of the T4 test; (e) sandbars' locations of the T5 test; (f) sandbars' locations of the T6 test; (g) sandbars' locations of the T7 test; (h) sandbars' locations of the T8 test. The red lines in the figure represent the sandbars, and the orange rectangles represent the flumes. The numbers at both ends of the red lines represent the distances between the two edges of sandbars and the dam toe, that is, the distances between the upstream and downstream edges of sandbars and the dam toe.

Growth characteristics of the upstream and downstream edges of the sandbars near the bed ends were similar to those of the sandbars near dam toes. That is, upstream edges grew toward dam toes, and the upstream edges move more extensively than the downstream edges. And sandbars downstream edges almost remained at the initial location. Sandbars' lengths gradually increased throughout the process of dam failure. Compared with the sandbars near the dam toes, the sandbars' movements in other reach were smaller. The distance between the sandbars in middle and end reach is smaller than the distance between sandbars near dam toe and adjacent sandbars.

The dam downstream slope and longitudinal section shape also influenced the sandbars. The largest movement distance for upstream edges of sandbars near the dam toe moved was 1.8 m, and for downstream edges of sandbars was 0.7 m with a downstream slope angle of 10° for trapezoidal shape models. It was the smallest movement distance for the upstream edge and the largest movement distance for the downstream edge for the trapezoidal shape models. The sandbar's final length was 1.2 m, which was the shortest among the downstream slope angle from 10 to 30°. However, sandbar length varied small with a maximum difference of 0.4 m when the angle increased from 15 to 30°. The lengths of sandbars in the middle and end reach were also the smallest for the 10° downstream slope. However, the distance between the sandbars was largest for the 10° downstream slope, and this is due to the smaller outburst flood discharge and capacity of bedload for the 10° downstream slope. The overlapping phenomena existed along the channel for sandbars with large downstream slope, such as the sandbars in the middle and end reach at 60 s for T2. For the triangular shape of the dam, the dam volume was the main factor influencing sandbars' developments. It could be demonstrated from two sides: one is the number of sandbars in the test, which dam downstream slope is 10° and with a larger dam volume, was more than the number of sandbars for 15 and 20° downstream slope dam models; the other is the lengths of sandbars in middle and end reaches become smaller with the increasing downstream slope from 10 to 20° (i.e., with decreasing dam volume).

3.3 Characteristics of the sandbars' geometric sizes

Corresponding to Sect. 3.2, Fig. 5 shows that the lengths of the sandbars near the dam toes were longer than other sandbars' lengths, and the sandbars near the dam toes appeared first. Because the sandbars near the dam toes were closer to the dams, when the flow carried a large number of sediments from the dam downstream slopes to the channel beds, the slopes decreased, and a large number of sediments accumulated around the sandbars near the dam toes to promote sandbars' developments. Sufficient incoming sand from the upper reach made the lengths of the sandbars near the dam toes

https://doi.org/10.5194/esurf-2020-92
Preprint. Discussion started: 16 December 2020

larger than the other sandbars' lengths. For all the sandbars, their lengths were largest in the whole process, followed by widths, and finally were heights. Sandbars' lengths had a growing trend, and their growth rates were more significant than growth rates of widths and heights. The sandbars' shapes were irregular during the entire dam failure process, which is similar to the field sandbars (Wu et al., 2020). The average values of the widths and heights of the entire sandbars were selected as the parameters reflecting the characteristics of sandbars' widths and heights shown in Fig. 5. From the figure, we can know that sandbars' widths changed more drastically than the sandbars' heights, which is mainly because sandbars' heights were significantly affected by outburst flow depth. In most cases, flow depth was less than the heights of sandbars, the sediments mostly accumulated at the sandbars' edges and waists, and could not "climb up" sandbars' tops; in addition, the reduction of flow depth was not large enough, so the sandbars' heights did not change much. The variations of widths and heights both increase slowly with time and then tended to be stable values.

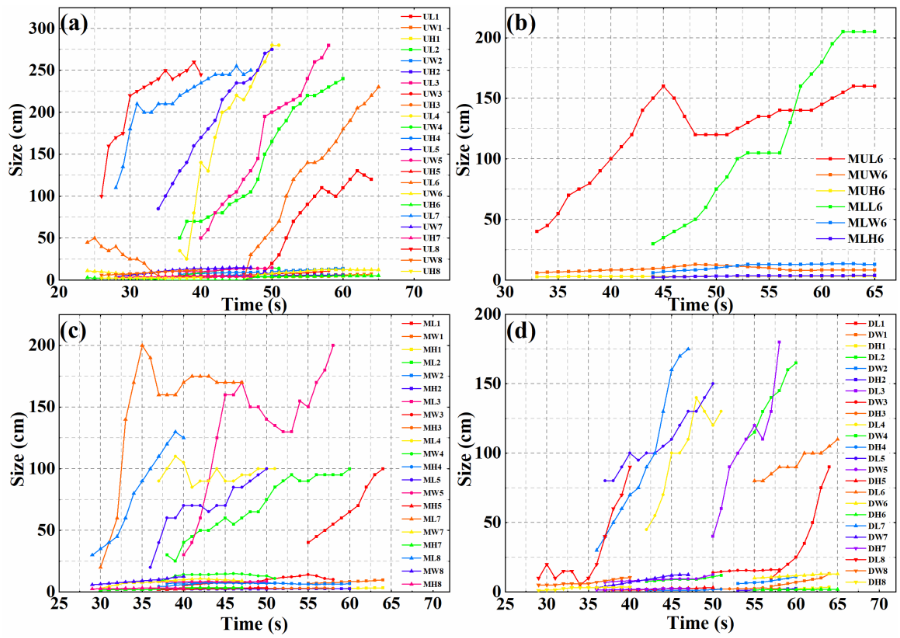

Figure. 5 The lengths, widths, and heights of the sandbars: (a) sizes of the sandbars near the dam toes; (b) sizes of the sandbars near the middle-upper and middle-lower reaches; (c) sizes of the sandbars near the middle reaches; (d) sizes of the sandbars near the bed ends. Notation: ULi, UWi, and UHi represent the length, width, and height of the sandbar near the dam toe of the Ti test, respectively. For example, UL1 indicates the length of the sandbar near the dam toe of the T1 test; MULi, MUWi, and MUHi represent the length, width, and height of the sandbar near the middle and upper reaches of the Ti test, respectively. For example, MUL1 indicates the length of the sandbar near the middle and upper reaches of the T1 test; MLi, MWi, and MHi represent the length, width, and height of the middle sandbar of the Ti test, respectively; MLLi, MLWi, and MLHi represent the length, width, and height of the sandbar near the middle and lower reaches of the Ti test, respectively; DLi, DWi, and DHi represent the length, width, and height of the sandbar near the bed end of the Ti test, respectively.

When the amounts of sediments deposited on sandbars were larger than the

https://doi.org/10.5194/esurf-2020-92
Preprint. Discussion started: 16 December 2020

quantities of eroded sediments, sandbars' volumes became larger. Otherwise, sandbars' volumes would decrease or remain at a stable level. Figure. 6 reveals sandbars' volume characteristics during the dam failure. Most of the 25 sandbars gradually increased in volume, indicating that the amounts of outburst flow erosions in the sandbars' vicinities were less than the amounts of siltation during the entire outburst process. The volumes were about 0.018 to 0.142, 0.009 to 0.055, and 0.014 to 0.055 times of the initial dam volumes for the sandbars near dam toes, the sandbars near the middle reaches, and the sandbars near the end reach, respectively. It indicates that sandbars' total volumes in the downstream channel of 4 to 7 times dam length to the initial dam volumes are about 0.009 to 0.142. By referring to Figs. 5 and 6, the sandbars' volume characteristics were consistent with the sandbars' length characteristics. And because the widths and heights developed in small change, sandbars' volumes were mainly controlled by sandbars' lengths.

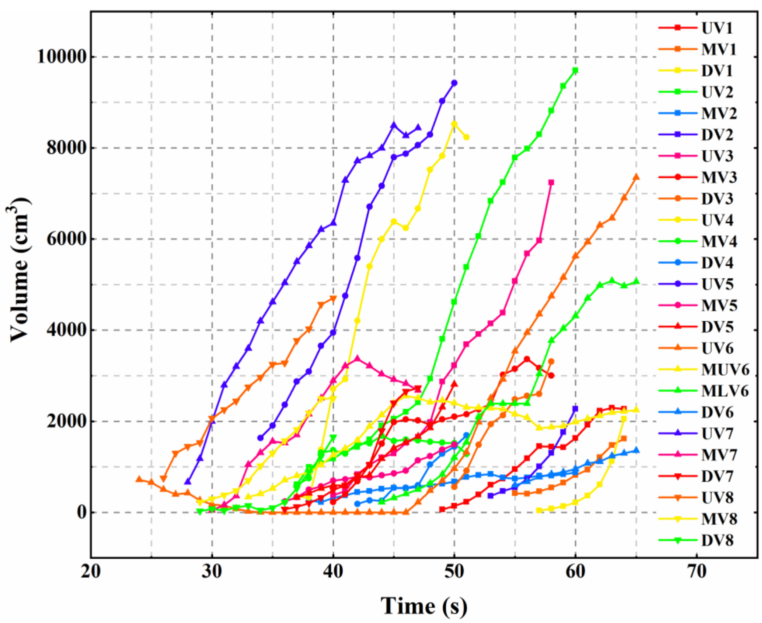

https://doi.org/10.5194/esurf-2020-92
Preprint. Discussion started: 16 December 2020

Earth Surface Dynamics Discussions
Open Access

Figure. 6 Volumes of sandbars. Notation: UVi, MVi, DVi, MUVi, MLVi represent the sandbar's volume near the dam toe, the sandbar near the middle reaches, the sandbar near the bed end, the sandbar near the middle-upper reaches, and the sandbar near the middle-lower reaches, respectively. For example, UV1 means that the sandbar's volume near the dam toe of the T1 test.

Jiang and Wei (2020) discussed the relationships between the lengths and the maximum widths and heights of sandbars when the dam was failed entirely, but the relationships with sandbars lengths, average widths, and heights had not been involved. It found that the average heights after the dam failure were about 1 to 3.5 times the maximum grain size. The ratios of lengths to average heights were basically between 10 to 80, and the rate of average widths to average heights were basically between 1 to 7 (Fig. 7).

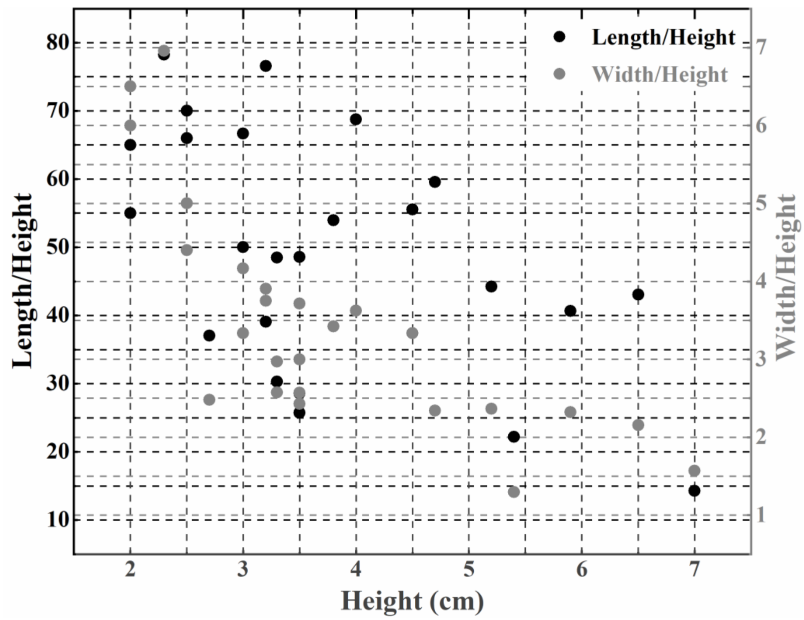

Figure. 7 The ratios of length and height, width and height of the sandbar at the end of the dam failure

https://doi.org/10.5194/esurf-2020-92
Preprint. Discussion started: 16 December 2020

4. Hydraulic characteristics of flow at the edges of the sandbars

Outburst flow influences the sandbars' formations and growths directly, and the existence of sandbars will also affect the outburst flow hydraulic characteristics. In order to understand how outburst flow affects sandbars' formations and developments, it is necessary to explore the outburst flow hydraulic characteristics.

As stated in Sect. 3, the sandbars' lengths are the most critical parameters affecting the sandbars' volumes, and sandbars' lengths are the most sensitive to the flow. Therefore, analyzing hydraulic parameters at the sandbars' upstream and downstream edges is helpful to understand the impact of the outburst flow on sandbars growths.

Sediment concentration in volume is an important physical parameter of sediment-laden flow and is closely related to sandbars growths. The concentration calculation method of Laursen (1958) was used to analyze the sediment concentrations in volumes at the sandbars' upstream and downstream edges. In order to facilitate the comparison of the sediment concentrations in volumes at the sandbars' edges, the average values of the sediment concentrations for the 25 sandbars' edges were taken (from the moment the sandbars were formed to the moment the dam was failed entirely), as shown in Fig. 8.

From Fig. 8, it reflects that average concentrations of the upstream edges of the sandbars near the dam toes are the largest, mainly because this location was close to the dam. Flow transported the dam materials to the vicinities of the sandbars near the dam toes, and the amounts of sediments transported were more than other parts of the channel bed. The sediment concentration of flow along the channel bed gradually decreased. The part of the sediments that caused the sediment concentration decreased to participate in sandbars' formations and growths. From the perspective of the entire sediment concentration variation range, there was a little difference between the concentrations at the upstream edges of the sandbars near the dam toes and the concentrations at the downstream edges of the sandbars near the bed ends, indicating that only a small part of sediments participated in the developments of the sandbars. The sediment concentrations of flow at the upstream and downstream edges of all sandbars had the same characteristic. The concentrations of flow at the upstream edges of sandbars were larger than that at the downstream edges. This was mainly because when the flow goes through the sandbars areas, some sediments deposit on the sandbars' upstream edges and abdomens, causing sandbars growths.

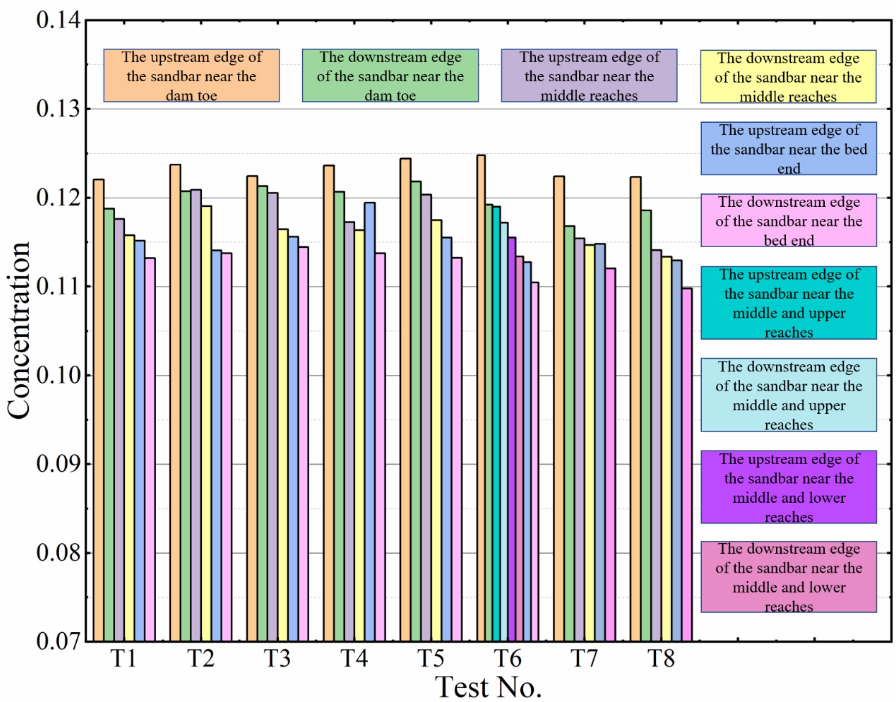

Figure. 8 Sediment concentrations in volumes at edges of sandbars

The ratio of the inertial force to the gravity of the outburst flow can be reflected by the Froude number (Fr). The equation for calculating the Froude number is as follow:

$$Fr = \frac{u}{\sqrt{gh}}, \tag{1}$$

where u is the flow velocity, m s^{-1}; g is the acceleration of gravity, m^2 s^{-1}; h is the flow depth, m.

In order to facilitate the comparison of the flow Froude numbers at different locations, the flow Froude numbers at the upstream and downstream edges of the 25 sandbars were taken as the average values over time of the entire dam failure process (from the moment the sandbar was formed to the moment when the dam was failed entirely), as shown in Fig. 9. It can be found that although the velocity and depth of flow in the late period of the peak discharge gradually decreased, the average Froude numbers of flow at the upstream and downstream edges of the sandbars are greater than 1, and it reflects the inertia effect is strong in these locations. If the streamline is changed in these locations, the particles in the water may move laterally or the original path causing sedimentation or erosion.

https://doi.org/10.5194/esurf-2020-92
Preprint. Discussion started: 16 December 2020

Earth Surface Dynamics
Discussions
Open Access
EGU

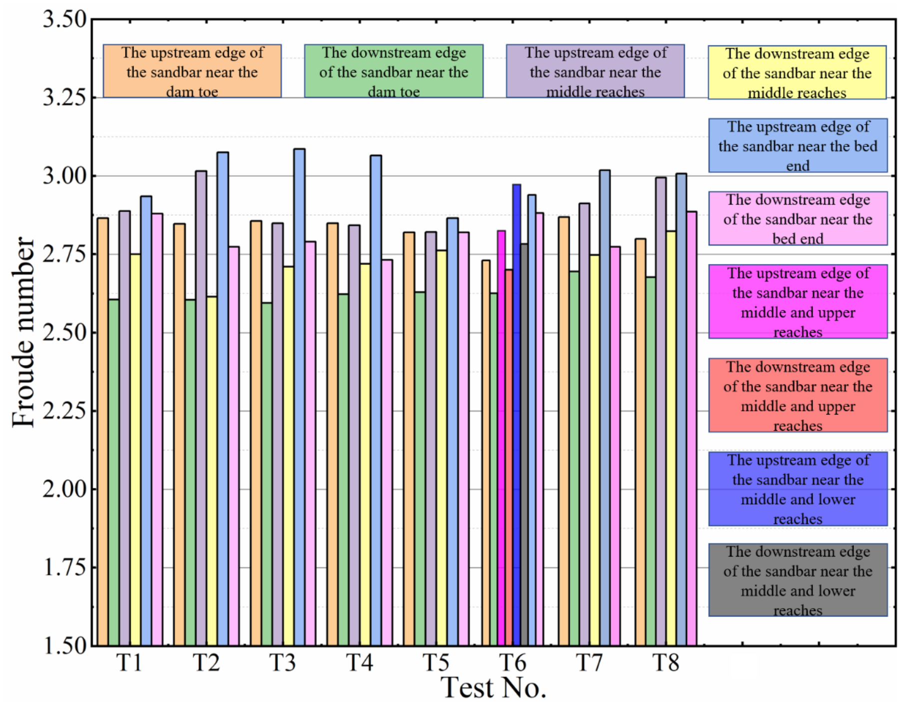

Figure. 9 Froude numbers of outburst flow at the edges of sandbars

The flow sediment carrying capacity indicates the amounts of sediments that can be carried through a river section under certain flow and boundary conditions. For these experiments, sandbars' formations and growths mainly depended on the accumulation of bedload, so we focused on the sediment carrying capacity of bedload. The calculation equation of bedload sediment carrying capacity is

$$c_e = \frac{q_b}{hu}, \tag{2}$$

where c_e is bedload sediment carrying capacity, q_b is the unit-width bedload transport rate, and it can be calculated using the MPM equation (Meyer-Peter, 1948)

$$q_b = 8\sqrt{(s-1)gd^3}(\theta-\theta_c)^{1.5}, \tag{3}$$

where θ is the Shields number, which can be obtained according to Eq. (4), and θ_c is the critical Shields number. Referring to Misri et al. (1984), θ_c is taken as 0.03 in this paper;

s is the submerged specific gravity of sediment, which can be calculated according to the Eq. (5); d is the particle size of the sediment, m.

$$\theta = \frac{u_*}{(s-1)gd}, \tag{4}$$

$$s = \frac{\rho_s}{\rho_w}, \tag{5}$$

where u_* is the frictional flow velocity, m s^{-1}; ρ_s is the weight of sediment, and ρ_w is the weight of water.

The volume of sediments that can be carried by the flow in the flow sections could be obtained with the above equations. Similarly, taking the average values of the sediment carrying capacities of flow (from the moment of sandbars formations to the moment of complete failure of the dam) for analysis, as shown in Fig. 10.

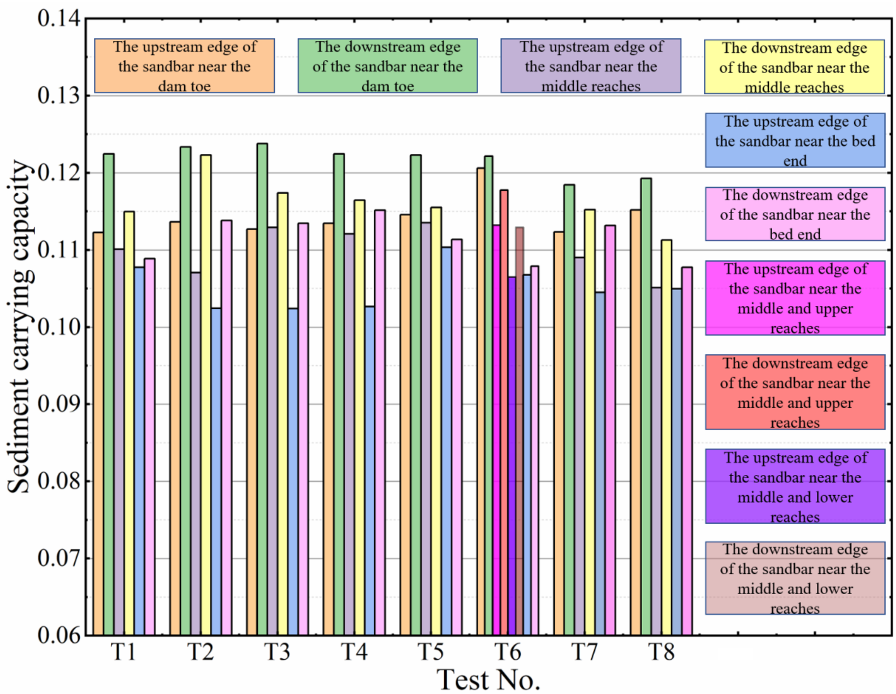

Figure. 10 Sediment carrying capacities of outburst flow at the edges of sandbars

https://doi.org/10.5194/esurf-2020-92
Preprint. Discussion started: 16 December 2020

It shows that, from the whole process's perspective, comparing the sediment carrying capacities at the upstream and downstream edges of different sandbars, the sediment carrying capacities decrease along the downstream channel bed. Taking the T1 test for example, the sediment carrying capacity of the flow at the upstream edge of the sandbar near the dam toe was larger than the sediment carrying capacity at the upstream edge of the sandbar near the middle reaches. The sediment carrying capacity at the downstream edge of the sandbar near the dam toe was larger than the sediment carrying capacity at the downstream edge of the sandbar near the middle reaches. The characteristic indicates that the outburst flow erosion effect gradually weakened with the distance from the dam. Compared to the sediment carrying capacities at the upstream and downstream edges of the same sandbar, it can be found that the sediment carrying capacity at the upstream edge was smaller than that at the downstream edge, but the difference was not large. Through combining Figs. 9 and 10, it can be found that there is a relationship between the sediment carrying capacity and the Froude number. That is, when the Froude number increases, the sediment carrying capacity will decrease; when the Froude number of the flow decreases, the sediment carrying capacity will increase.

5. The influence of outflow transportation capacity on development of sandbars' lengths

Sandbar length is the predominant factor to control the volume. The transportation condition of outflow at the sandbars' edges determines sandbar growth: for the sandbars'

https://doi.org/10.5194/esurf-2020-92
Preprint. Discussion started: 16 December 2020

upstream edges, if the sediment concentrations in volumes are greater than the sediment carrying capacities of the flow, sediments are accumulated, and the upstream edges will extend toward the dam toes. And suppose the sediment concentrations in volumes are less than the flow sediment carrying capacities. In that case, the upstream edges of sandbars will be in a state of erosion, and the sandbars' upstream edges will extend far away from the dam toes. As for the sandbars downstream edges, when the sediment carrying capacities of the flow are smaller than the sediment concentrations, it means that the flow cannot take away all sediments. Sediments will deposit, and the downstream edges of sandbars will extend far from the dam toes; when the sediment carrying capacities are larger than the sediment concentrations, the downstream edges of the sandbars will be in an eroded state, and the sediments are carried by flow to the downstream channel bed, and the sandbars' downstream edges will extend toward the dam toes; when the sediment carrying capacities of the flow are equal to the sediment concentrations, then the flow at sandbars' downstream edges will be in an equilibrium sediment transport state. Figure. 11 shows the relationships between the sediment concentrations in volumes and the sediment carrying capacities at the sandbars upstream and downstream edges. It can be seen that the differences between the sediment concentrations in volumes and the sediment carrying capacities (c-c_e) fluctuate during the whole process of sandbars developments. Through referring to Figs. 4 and 11, the two pictures are highly consistent. When the (c-c_e) in Fig. 11 is greater than 0, the sandbar's upstream edge point migrates upstream, or the downstream edge point of the sandbar migrates downstream in Fig. 4. When the (c-c_e) is less than 0, the

https://doi.org/10.5194/esurf-2020-92
Preprint. Discussion started: 16 December 2020

sandbar's upstream edge point migrates downstream, or the downstream edge point of the sandbar migrates upstream.

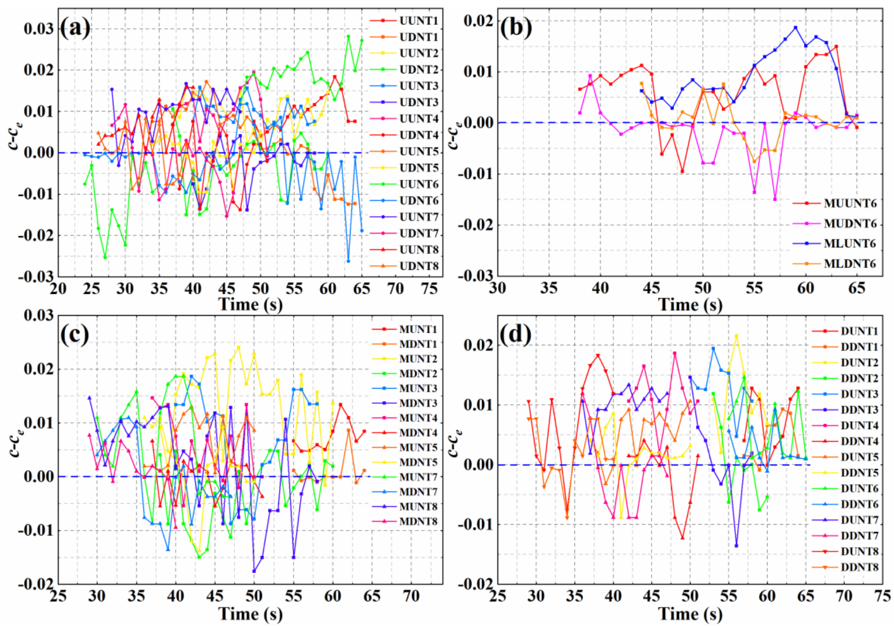

Figure. 11 The difference of the sediment concentrations in volumes and the sediment carrying capacities (c-c_e) at upstream and downstream edges of sandbars: (a) the (c-c_e) at the edges of the sandbars near the dam toes; (b) the (c-c_e) at the edges of the sandbars near the middle and upper reaches; (c) the (c-c_e) at the edges of the sandbars near the middle reaches; (d) the (c-c_e) at the edges of the sandbars near the bed ends. Notation: c is the sediment concentration in volume; c_e is the sediment carrying capacity of flow; UUNTi, UDNTi represent (c-c_e) at the upstream and downstream edges of the sandbar near the dam toe of the Ti test. For example, UUNT1 represent the value of (c-c_e) at the upstream edge of the sandbar near the dam toe of the T1 test; MUUNTi, MLDNTSi represent (c-c_e) at the upstream and downstream edges of the sandbar near the middle and upper reaches of the Ti test; MLUNTi, MLDNTSi represent (c-c_e) at the upstream and downstream edges of the sandbar near the middle and lower reaches of the Ti test; MUNTi, MDNTSi

https://doi.org/10.5194/esurf-2020-92
Preprint. Discussion started: 16 December 2020

represent (c-c_e) at the upstream and downstream edges of the sandbar near the middle reaches of the Ti test; DUNTi, DDNTi represent (c-c_e) at the upstream and downstream edges of the sandbar near the bed end of the Ti test. (i=1 to 8)

The sums of (c-c_e) at the sandbars' upstream and downstream edges are used as the criterion for judging the sandbars' length variation. The relationships between the sums of (c-c_e) and zero determine the increase or decrease of sandbars' lengths. Suppose the sums of (c-ce) are greater than zero. In that case, it means that the outburst flow cannot transport all the sediments. The excess sediments are deposited in the sandbars areas, corresponding to the increase in sandbars' lengths and volumes; otherwise, sandbars' lengths and volumes are reduced. Figure. 12 shows the relationships between the sums of (c-c_e) at the sandbars' edges and 0. By combining Figs. 12 and 6, it can be seen that when the sums of (c-c_e) are greater than 0, sandbars' lengths and volumes are increased. It reveals that the relationship between the sums of (c-c_e) and 0 can be used to judge the trend of sandbars' lengths and volumes.

https://doi.org/10.5194/esurf-2020-92
Preprint. Discussion started: 16 December 2020

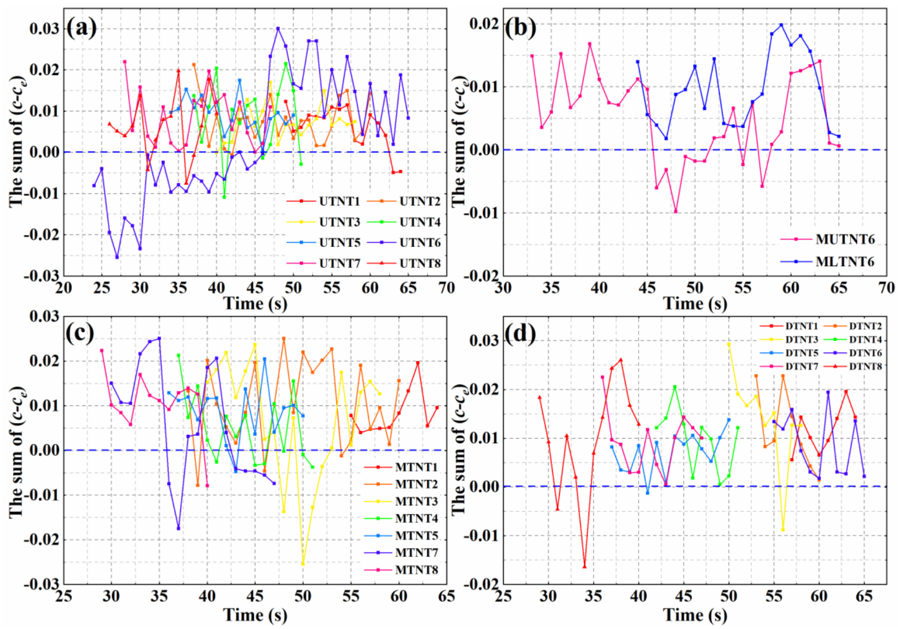

Figure. 12 The sums of (c-c_e) at the upstream and downstream edges of sandbars: (a) the sums of (c-c_e) at the upstream and downstream edges of the sandbars near the dam toes; (b) the sums of (c-c_e) at the upstream and downstream edges of the sandbars near the middle-upper reaches, and the sandbars near the middle-lower reaches; (c) the sums of (c-c_e) at the upstream and downstream edges of the sandbars near the middle reaches; (d) the sums of (c-c_e) at the upstream and downstream edges of the sandbars near the bed ends. Notation: for the Ti test, UTNTi, MUTNTi, MLTNTi, MNTTi, DTNTi respectively represent the sum of the (c-c_e) at the upstream and downstream edges of the sandbar near the dam toe, the sandbar near the middle-upper reaches, the sandbar near the middle-lower reaches, and the sandbar near the middle reaches, and the sandbar near the bed end. (i=1 to 8)

6. Conclusion

In this paper, a downstream moveable bed with 4 to 7 times the length of dam

https://doi.org/10.5194/esurf-2020-92
Preprint. Discussion started: 16 December 2020

length along the channel was set, and through eight flume experiments, 25 sandbars were formed downstream channel caused by overtopping flow. The sandbars development characteristics and the influences of hydraulic parameters on sandbars were also analyzed. The main conclusions are as follows.

(1) The number of sandbars is 0.4 to 1.0 times the ratio of river bed length to dam length. Sandbars first appeared near dam toes located on the dam breach sides across the rivers. Inertia force made sediment accumulate on the opposite banks of the channel bed, resulting in the formations of sandbars downstream. Meanwhile, it has the characteristic that the farther away from the dam, the later the sandbar formation. During the evolution of outburst flow, the sandbars' upstream edges are mainly in siltation states. The sandbars' lengths increase with failure time, mainly caused by sandbars' upstream edges move upstream. The downstream edges develop slowly and basically near the initial positions. And the developments of sandbars downstream edges are much smaller than the developments of sandbars' upstream edges.

(2) During dam failure, the lengths varied faster than the widths and heights of sandbars. And the lengths along the river are the largest, followed by widths, and finally are sandbars' heights after the dam failure. The average sandbars' heights are about 1 to 3.5 times the maximum particle size. The sandbars' lengths are about 10 to 80 times the average heights, and the average widths are 1 to 7 times the average heights. The lengths mainly control the sandbars' volumes. The ratio of sandbars' total volumes in the downstream channel of 4 to 7 times dam length to initial dams' volumes are about 0.009 to 0.142.

https://doi.org/10.5194/esurf-2020-92
Preprint. Discussion started: 16 December 2020

(3) The impact of outburst flow on sandbars is mainly manifested by the sediment concentration and the sediment carrying capacity. During the entire dam failure process, the sediment concentrations at sandbars' upstream edges are greater than that on the downstream edges. The Froude number has a significant influence on the sediment carrying capacity. When the Froude number increases or decreases, the sediment carrying capacity decreases or increases accordingly. The sediment carrying capacities at the sandbars' upstream edges are smaller than those at the sandbars' downstream edges. The characteristics of sediment concentrations and sediment carrying capacities at sandbars' edges cause sandbars to develop upstream.

(4) The formation processes and development characteristics of sandbars from the perspective of flow transporting sediments are analyzed. There is a corresponding good relationship between outburst flow hydraulic characteristics and sandbars development characteristics: the difference between the sediment concentration and the sediment carrying capacity of the flow will determine the erosion and accumulation of sediments that affect sandbars developments. The sandbars developments are an intuitive manifestation of the changes in outburst flow hydraulic characteristics.

Author contribution

Xiangang Jiang was responsible for the experiments, article thinking, and writing. Haiguang Cheng was responsible for calculating the article parameters. Lei Gao was responsible for the article's pictures, and Weiming Liu was responsible for checking the full article.

https://doi.org/10.5194/esurf-2020-92
Preprint. Discussion started: 16 December 2020

Earth Surface Dynamics Discussions
Open Access

Competing interests

The authors declare that they have no known competing financial interests or personal relationships that could have appeared to influence the work reported in this paper.

Acknowledgments

This research has been supported by The National Natural Science Foundation of China (No. 41807289) and Key Laboratory of Ministry of Education for Geomechanics and Embankment Engineering, Hohai University (No. 202020) and Open fund of Key Laboratory of mountain hazards and surface processes, Chinese Academy of Sciences (No. KLMHESP-20-05).

Code and data availability statement

The codes and data that support the findings of this study are available from the corresponding author upon reasonable request.

Reference

Alexander, J. S., Mcelroy, B., Huzurbazar, S., Elliott, C., and Murr, M. L.: Deposition potential and flow-response dynamics of emergent sandbars in a braided river, Water Resources Research, 56, 1, n/a-n/a, https://doi.org/10.1029/2018WR024107, 2020.

Ashworth, and Philip J.: Mid-channel bar growth and its relationship to local flow

https://doi.org/10.5194/esurf-2020-92
Preprint. Discussion started: 16 December 2020

strength and direction, Earth Surf Proc Land, 21, 2, 103-123, https://doi.org/10.1002/(SICI)1096-9837(199602)21:2<103::AID-ESP569>3.0.CO;2-O, 1996.

Ashworth, P. J., Best, J. L., Roden, J. E., Bristow, C. S., and Klaassen, G. J.: Morphological evolution and dynamics of a large, sand braid-bar, Jamuna River, Bangladesh, Sedimentology, 47, 3, 533-555, https://doi.org/10.1046/j.1365-3091.2000.00305.x, 2000.

Chen, S. C., Lin, T. W., and Chen, C. Y.: Modeling of natural dam failure modes and downstream riverbed morphological changes with different dam materials in a flume test, Engineering Geology, 188, 148-158, https://doi.org/10.1016/j.enggeo.2015.01.016, 2015.

Chien N., Zhang R., and Zhou Z. D.: Fluvial processes, Bei jing: Science Press (in Chinese).

Costa, J. E., and Schuster, R. L.: The formation and failure of natural dams, Geol Soc Am Bull, 100(7), 1054-1068, https://doi.org/10.1130/0016-7606(1988)100<1054:TFAFON>2.3.CO;2, 1988.

Crosato, A., and Mosselman, E.: Simple physics-based predictor for the number of river bars and the transition between meandering and braiding. Water Resour Res, 45, 3, n/a-n/a, https://doi.org/10.1029/2008wr007242, 2009.

Defina, A.: Numerical experiments on bar growth. Water Resour Res, 39, 4, 285-285, https://doi.org/10.1029/2002WR001455, 2003.

Demirci, M., Aköz, M. S., and Üneş, F.: Experimental investigation of cross-shore

https://doi.org/10.5194/esurf-2020-92
Preprint. Discussion started: 16 December 2020

sandbar volumes. J Coast Conserv, 18, 1, 11-16, https://doi.org/10.1007/s11852-013-0289-5, 2014.

Fan, X. M., Tang, C. X., van Westen, C. J., and Alkema, D.: Simulating dam-breach flood scenarios of the Tangjiashan landslide dam induced by the Wenchuan Earthquake, Natural Hazards and Earth System Science, 12, 10, 3031-3044, https://doi.org/10.5194/nhess-12-3031-2012, 2012.

Gao, J.: On the formation of shoal in river, J Hydraul Eng, 6, 6, 66-70 (in Chinese), https://doi.org/10.3321/j.issn:0559-9350.1999.06.013, 1999.

Hooke, J. M., and Yorke, L.: Channel bar dynamics on multi-decadal timescales in an active meandering river, Earth Surface Processes and Landforms, 36, 14, 1910-1928, https://doi.org/10.1002/esp.2214, 2011.

Jiang, X. G., Cui, P., Chen, H. Y., and Guo, Y. Y.: Formation conditions of outburst debris flow triggered by overtopped natural dam failure, Landslides, 14, 3, 821-831, https://doi.org/10.1007/s10346-016-0751-1, 2017.

Jiang, X. G., Huang, J. H., Wei, Y. W., Niu, Z. P., Chen, F. H., Zou, Z. Y., and Zhu, Z. Y.: The influence of materials on the breaching process of natural dams, Landslides, 15(2), 243-255. https://doi.org/10.1007/s10346-016-0751-1, 2018.

Jiang, X. G., Wei, Y. W., Wu, L., Hu, K. H., Zhu, Z. Y., Zou, Z. Y., and Xiao, W. M.: Laboratory experiments on failure characteristics of non-cohesive sediment natural dam in progressive failure mode, Environmental Earth ences, 78, 17, 1-14, https://doi.org/10.1007/s12665-019-8544-1, 2019a.

Jiang, X. G., and Wei, Y. W.: Natural dam breaching due to overtopping: Effects of

https://doi.org/10.5194/esurf-2020-92
Preprint. Discussion started: 16 December 2020

initial soil moisture, B Eng Geol Environ, https://doi.org/10.1007/s10064-018-01441-7, 2019b.

Jiang, X. G., and Wei, Y. W.: Erosion characteristics of outburst floods on channel beds under the conditions of different natural dam downstream slope angles, Landslides, 1-12, https://doi.org/10.1007/s10346-020-01381-y, 2020.

Kobayashi, Kensuke, Shimizu, Yasuyuki, and Watanabe, Yasuharu.: Morphodynamic modeling of sandbar evolution under unsteady flow, Journal of Applied Mechanics, 1031, 2010.

Laursen, E. M.: The total sediment load of streams, Journal of the Hydraulics Division, 84, 1, 1-36, 1958.

Lin, C. K.: The construction of the Shanghai port and its sea-entering channel, influenced by the sediments and the fluvial processes at the Changjiang River Estuary and the Hangzhou Wan, Acta Geographica Sinica, 45, 78-89 (in Chinese), 1990.

Meyer-Peter, E., and Müller, R.: Formulas for bedload transport, Proc of Congress Iahr 3, http://dx.doi.org/, 1948.

Misri, R. L., Garde, R. J., and Raju, K. G. R.: Bed load transport of coarse nonuniform sediment, J Hydraul Eng, 110, 3, 312-328, https://doi.org/10.1061/(ASCE)0733-9429(1984)110:3(312), 1984.

Mueller, E. R., and Grams, P. E.: Modeling decadal changes in sandbar volume using sub-daily records of flow and sand concentration downstream from a large dam, In Joint Rocky Mountain Gsa Section, https://doi.org/10.1130/abs/2018RM-

314039, 2018.

Peng, M., and Zhang, L.M.: Breaching parameters of landslide dams, Landslides, 9, 1, 13-31, https://doi.org/10.1029/2018WR024107, 2012.

Pickert, G., Weitbrecht, V., and Bieberstein, A.: Breaching of overtopped river embankments controlled by apparent cohesion, J Hydraul Res, 49, 2, 143-156, https://doi.org/10.1080/00221686.2011.552468, 2011.

Takahashi, T.: Debris flow Mechanics, Prediction and Countermeasures, Taylor and Francis Group, 35-38, https://doi.org/10.1201/9780203946282, 2007.

Tracy-Smith, E., Galat, D. L., and Jacobson, R. B.: Effects of flow dynamics on the aquatic-terrestrial transition zone (ATTZ) of Lower Missouri River sandbars with implications for selected biota, River Res Appl, 28, 7, 793-813, https://doi.org/10.1002/rra.1492, 2012.

Turzewski, M. D., Huntington, K. W., and Leveque, R. J.: The Geomorphic Impact of Outburst Floods: Integrating Observations and Numerical Simulations of the 2000 Yigong Flood, Eastern Himalaya, Journal of Geophysical Research: Earth Surface, 124, 5, https://doi.org/10.1029/2018JF004778, 2019.

Wright, S. A., and Kaplinski, M.: Flow structures and sandbar dynamics in a canyon river during a controlled flood, Colorado River, Arizona, Journal of Geophysical Research Earth Surface, 116, F1, n/a-n/a, https://doi.org/10.1029/2009jf001442, 2011.

Wu C. H., Hu, K. H., Liu, W. M., Wang, H., Hu, X. D., and Zhang, X. P.: Morpho-sedimentary and stratigraphic characteristics of the 2000 Yigong River landslide

https://doi.org/10.5194/esurf-2020-92
Preprint. Discussion started: 16 December 2020

Earth Surface Dynamics
Discussions
Open Access

dam outburst flood deposits, eastern Tibetan Plateau, Geomorphology, 107293, https://doi.org/10.1016/j.geomorph.2020.107293, 2020.

Xie, D. F., Gao, S., Wang, Z. B., Pan, C. H., Wu, X. G., and Wang, Q. S.: Morphodynamic modeling of a large inside sand bar and its dextral morphology in a convergent estuary: Qiantang Estuary, China, Journal of Geophysical Research: Earth Surface, 122, https://doi.org/10.1002/2017JF004293, 2017.

Zhang, L. M., Xiao, T., He, J., and Chen, C.: Erosion-based analysis of breaching of Baige landslide dams on the Jinsha River, China, in 2018, Landslides, 1965–1979, https://doi.org/10.1007/s10346-019-01247-y, 2019.

Zhou, G. G. D., Zhou, M. J., Shrestha, M. S., Song, D. R., Choi, C. E., Cui, K. F. E., Peng, M., Shi, Z. M., Zhu, X. H., and Chen, H. Y.: Experimental investigation on the longitudinal evolution of landslide dam breaching and outburst floods, Geomorphology, 334, 29-43, https://doi.org/10.1016/j.geomorph.2019.02.035, 2019.